



# A new approach to design of RF energy harvesting system to enslave wireless sensor networks

Alex Mouapi<sup>a,\*</sup>, Nadir Hakem<sup>a</sup>, Gilles Y. Delisle<sup>a,b</sup>

<sup>a</sup> *Underground Communications Research Laboratory, University of Quebec in Abitibi-Témiscamingue (UQAT), Val d'Or, Québec, Canada J9P 1Y3*

<sup>b</sup> *Department Of Electrical and Computer Engineering, Laval University, Québec City, Canada G1V 0A6*

Received 20 January 2017; accepted 9 November 2017

Available online 23 December 2017

## Abstract

In trying to reach the goal of controlling the environment, recent years have seen the rapid emergence of Wireless Sensors Networks (WSN). Nevertheless, the lifetime of sensor nodes shows a strong dependence on battery capacity. Recently energy harvesting techniques have been considered to allow the use of WSN in the “deploy and forget” mode. This paper proposes an assessment of the performance of a WSN enslaved to an optimized Radiofrequency Energy Harvesting System (REHS). The energy budget of a sensor node in a Low-Energy Adaptive Clustering Hierarchy (LEACH) protocol is quantified and used to evaluate the performance of the WSN.

© 2017 The Korean Institute of Communications Information Sciences. Publishing Services by Elsevier B.V. This is an open access article under the CC BY-NC-ND license (<http://creativecommons.org/licenses/by-nc-nd/4.0/>).

**Keywords:** Energy harvesting; LEACH protocol; REHS; WSN

## 1. Introduction

The smart city concept is increasingly used to integrate the Information and Communications Technology (ICT) in the urban environment. Thus, public access terminals in Wireless-Fidelity (Wi-Fi) and the Wireless Sensors Network (WSN) have numerous applications that improve people lives. Particularly, WSNs are increasingly used in several applications; this includes but not limited to structural monitoring [1], habitat monitoring [2], health monitoring [3] and Internet of Things (IoT) environment [4]. A major constraint in the deployment of a WSN is its energy dependence since sensor nodes are battery powered and thus have very limited energy capacity. In some cases, maintenance operations that include battery replacement or recharge may be costly. For applications such as IoT (in the building monitoring), battery replacement may not be possible. Recently, the energy harvesting technique which consists of

converting a primary energy source (i.e. light, vibration, airflow, electromagnetic waves, heat) into DC energy – that is directly usable by the sensor node – has been considered as a solution for battery recharge [5]. Energy harvesting techniques differ from one another by the nature of the used primary source. A comparison of the various sources and necessary dimensions to acquire sufficient energy is presented in Table 1 [6]. The RF energy harvesters is shown to have smaller dimensions compared to the other harvesters. This is an advantage for miniature applications.

The main objective of this work is to improve sensor nodes’ life for applications in remote areas. The used solution proposes to enslave the node to the ubiquitous RF energy source. The enslavement involves determining the network size, the type of physical phenomenon that can be measured, and the range of the WSN. To achieve this objective, the proposed method compares the amount of the recoverable energy from the electromagnetic waves to the energy requirement of the sensor node during an operating cycle. The conceptual view of the problem is shown in Fig. 1. An antenna combined with a rectifying circuit known as rectifying antenna (rectenna) is used

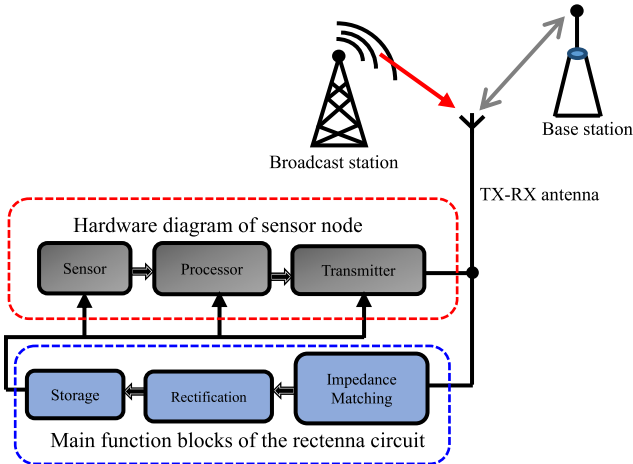
\* Corresponding author.

E-mail addresses: [alex.mouapi@uqat.ca](mailto:alex.mouapi@uqat.ca) (A. Mouapi), [nadir.hakem@uqat.ca](mailto:nadir.hakem@uqat.ca) (N. Hakem), [gilles.delisle@gel.ulaval.ca](mailto:gilles.delisle@gel.ulaval.ca) (G.Y. Delisle). Peer review under responsibility of The Korean Institute of Communications and Information Sciences (KICS).

**Table 1**

Comparison of energy harvesting techniques for wireless sensor networks [6].

Energy sources	Performance	Necessary dimension
Airflow	0.4–1 mW/cm <sup>3</sup>	6–15 cm <sup>3</sup>
Light (indoor)	10–100 μW/cm <sup>3</sup>	59–590 cm <sup>2</sup>
Vibrations	200–380 μW/cm <sup>3</sup>	16–30 cm <sup>3</sup>
Thermoelectric	40–60 μW/cm <sup>2</sup>	98–148 cm <sup>2</sup>
Electromagnetic waves	0.2–1 mW/cm <sup>2</sup>	6–30 cm <sup>2</sup>

**Fig. 1.** Conceptual view of enslaved sensor node.

to harvest energy from electromagnetic waves. This energy is then used to power the wireless sensor node whose function is the collection, processing, and transmission of environmental data (such as temperature, pressure and humidity). Considering the principle of reciprocity of antennas, the same antenna is used for data transmission and for recovering the surrounding ambient energy.

Based on the purpose of this work, this letter is organized as follows: in Section 2, a consumption model for a sensor node is proposed. Assuming that the amount of the available RF energy is the same throughout the WSN, the Low-Energy Adaptive Clustering Hierarchy (LEACH) protocol is considered in this work; this allows a fair distribution of the WSN loads to the different nodes it contains [7]. Section 3 presents the experimental results from the design of a miniature and highly efficient rectenna. The electrical output characteristics of the rectenna are then used to evaluate the performance of the WSN enslaved to RF energy. Finally Section 4 concludes the letter.

## 2. Energetic budget of a sensor node in LEACH clustering WSN

Since a WSN lifetime is dependent on the lifetime of individual sensor nodes [7,8], efficient utilization of each node's energy is a vital issue. In this context, the LEACH protocol allows the different nodes of the WSN to have fair loads, this through a permutation of the cluster head in each round. This idea was first proposed in [7], and the basic concept was to transmit data from sensor nodes, through its cluster head, to the base station in rounds. In each round, a random Cluster Head

(CH) selection mechanism is performed. Each round consists of two phases, the set-up phase, and the steady phase. In the set-up phase, each node decides whether or not to become a cluster head for the current round. In the steady phase, the cluster heads collect data from ordinary nodes, aggregate the data and send it to the BS.

To define the energy requirement of a sensor node, the following reasonable assumptions are made:

- only the energy consumed during the steady phase is considered [7];
- only the energy used to transmit and receive the data is considered [9];
- all sensor nodes are homogeneous; the sensor nodes measure the same amount of data and are all located at an average distance  $d_1$  from the CH;
- the fixed BS is located far from the sensor field. Thus all CHs are approximately at the same  $d_2$  distance from the BS;
- the Friis space model is considered for communication inside cluster while the multipath fading model will be used for communication between the CH and the base station [7];
- the clusters are circular in shape and are all the same size: the WSN includes  $N$  uniformly distributed sensors in a region of surface  $M^2$ . Each cluster includes  $N/k$  nodes on a surface  $M^2/k$  [10];
- all sensor nodes within a cluster use time division multiple access (TDMA) to access their CH [10];
- a perfect aggregation of data is made in the CH [7].

In all the analysis, the same radio model used in [7,8] is considered. Readers are referred to these references for more details.

Once collected measures, an Ordinary Node (ON) just have to transmit them to the CH. Then the dissipated energy per round in ON is expressed as:

$$E_{ON}(\ell, d_1) = \ell (E_{elec} + \varepsilon_{fs} \cdot d_1^2) \quad (1)$$

where  $E_{elec}$  is the energy consumption per bit in the transmitter and receiver circuitry and  $\varepsilon_{fs}$  is the multiple attenuation model amplifier energy consumption. If the CH is assumed to be the center of mass of the cluster, the expected squared distance from the nodes to the cluster head  $d_1^2$  is defined as [7]:

$$E[d_1^2] = M^2/2\pi k \quad (2)$$

Substituting Eq. (2) into Eq. (1) gives:

$$E_{ON}(\ell, k, M) = \ell (E_{elec} + \varepsilon_{fs} \cdot M^2/2\pi k) \quad (3)$$

The CHs have to collect data from ONs, aggregate the data and send it to the BS. Thus, the energy budget of the CH is defined by:

$$E_{CH} = \ell (N/k - 1) E_{elec} + \frac{\ell E_{DA} N}{k} + \ell (E_{elec} + \varepsilon_{amp} \cdot d_2^4) \quad (4)$$

where  $E_{DA}$  is the energy for data aggregation [7].

The energy dissipated in a cluster per round can be defined by:

$$E_{\text{Cluster}} = (N/k - 1) E_{\text{ON}} + E_{\text{CH}} \quad (5)$$

and the total energy per round is  $E_{\text{total}} = k E_{\text{Cluster}}$ . Since the total network load is distributed evenly among all nodes, we deduce then that the average consumption of the node per round is defined by:

$$E_{\text{node}} = E_{\text{total}}/N \quad (6)$$

Substituting Eqs. (3) and (5) into Eq. (6) and by differentiating the resulting equation with respect to  $k$  and equating to zero, the resulting optimal number of cluster,  $k_{\text{opt}}$  is:

$$k_{\text{opt}} = M \sqrt{\varepsilon_{fs}} \sqrt{N} / \sqrt{2\pi (\varepsilon_{amp} \cdot d_2^4 - E_{\text{elec}})} \quad (7)$$

The minimum consumption of the node will be defined by:

$$E_{\text{total}_{\min}} = (k E_{\text{Cluster}}/N)|_{k=k_{\text{opt}}} \quad (8)$$

In the continuation of this work, the  $d_{CH-BS}$  parameter will be used to enslave the sensor node to a rectenna designed to achieve optimal performance in the 2.45 GHz frequency band.

### 3. High efficiency miniature rectifier design for Rf energy harvesting at 2.45 GHz

In the design of wireless sensor nodes, most of the used radio modules operate at 2.45 GHz [6]. This section then proposes a design methodology for a miniature and highly efficient rectifier circuit for applications in the ISM band centralized at 2.45 GHz. Given the random input RF power, it is important to optimize the harvesting circuit to have a minimum of usable energy. In this work, optimization will be to design a high efficient rectifier circuit. The design methodology is based on a judicious choice of the rectifying diode which in addition to having the best conversion efficiency should be highly sensitive in order to detect low ambient RF power levels.

#### 3.1. Rectifier diode selection

The sensitivity of the rectifier circuit whose role is to convert the harvested RF signals into a DC signal is directly related to the sensitivity of the used rectifying diode [11]. Then, the influencing factor on rectenna efficiency is diode efficiency and a significant portion of the losses on rectenna circuit provided by the diodes electrical parameters. Considering the high frequency of the signals, fast switching Schottky diodes are the most used in the design of the rectifier's circuits. A non-exhaustive list of recently used rectifier diodes is given in Table 2.

Evaluation of the conversion efficiency of a Schottky diode using equivalent circuit of the diode with a resistive load  $R_L$  shown in Fig. 2 has been proposed in [12] and it is now a classical.

Considering diode's characteristics given in Table 1, this well-known approach [12] has been used to compare the efficiencies of the different diodes at 2.45 GHz. The result is shown in Fig. 3(a) and it is observed that the HSMS 2850 and HSMS

**Table 2**  
Commonly used diodes [10].

Diodes	HSMS 2810	HSMS 2820	HSMS 2850	HSMS 8101
$C_{j0}$ (pF)	1.1	0.7	0.18	0.26
$R_s$ ( $\Omega$ )	10	6	25	14
$V_j$ (V)	0.65	0.65	0.35	0.35

$C_{j0}$  is diode's zero bias junction capacitance.

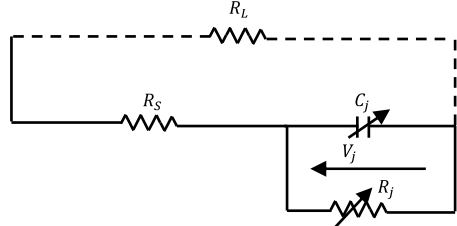


**Fig. 2.** Small signal model of a Schottky diode [12].

8101 diodes show the best efficiencies compared to the other considered diodes. To select the rectifier diode, a comparison of the detection threshold of these two diodes is proposed in Fig. 3(b). The analysis is conducted using ADS (Advanced Design System) simulation version 2014. The curve shows that the HSMS 2850 diode can detect very low power levels. It is this diode which will be considered to design the rectifier circuit.

#### 3.2. Experimental validation

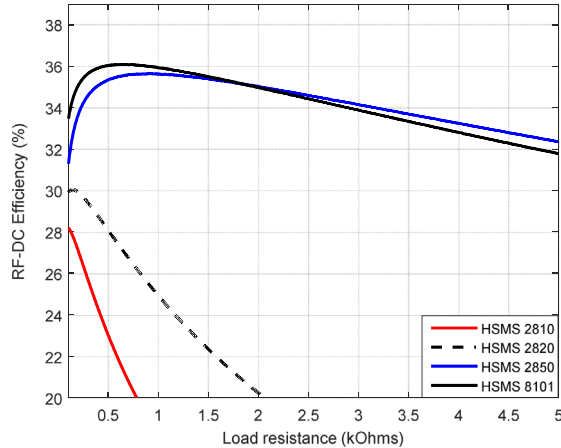
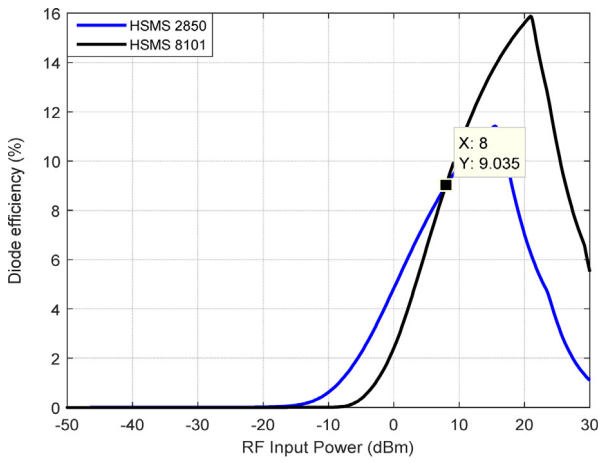
An experimental validation of the designed rectifier circuit has been implemented. Several topologies of rectifier are commonly used: single serial or shunt diode, voltage doubler and bridge circuit [10]. The voltage doubler (Fig. 6) is used here since it has the advantage of achieving higher output voltage than other topologies for the same RF input power. The corresponding fabricated circuit is shown in Fig. 4. To realize the circuit, an RO350B substrate ( $\varepsilon_r = 3.48$ ,  $h = 0.76$  mm,  $T = 35$   $\mu$ m,  $\tan \delta = 0.0037$ ) of Rogers Corporation was chosen. A SubMiniature version A (SMA) connector is used to connect the rectifier to the microwave source.

The experimental setup shown in Fig. 4 is used. It includes an Anritsu microwave source MG3700A with an impedance internal  $50 \Omega$  and able to transmit signals up to 6 GHz.

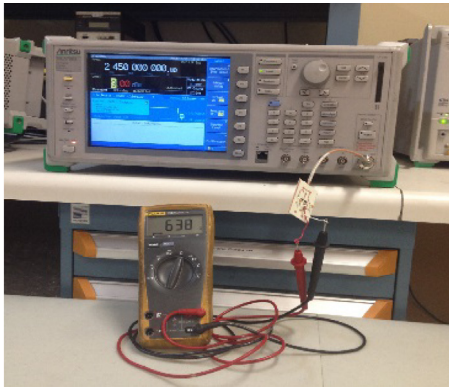
The experimental results shown in Fig. 5 are easily comparable to the simulated results. A slight distortion is observed on the experimental curve due to the fact that the parasitic elements of the housing are not taken into account in the simulation.

#### 3.3. Rectifier performances improvement

A matching circuit must be placed between the microwave source and the rectifier to ensure optimum power transfer (Fig. 1). In this work, the ADS 2014 impedance matching tool is used to size the filter. This tool allows us to place a component in our scheme and, according to certain parameter manually defined, generated a matching circuit which can then

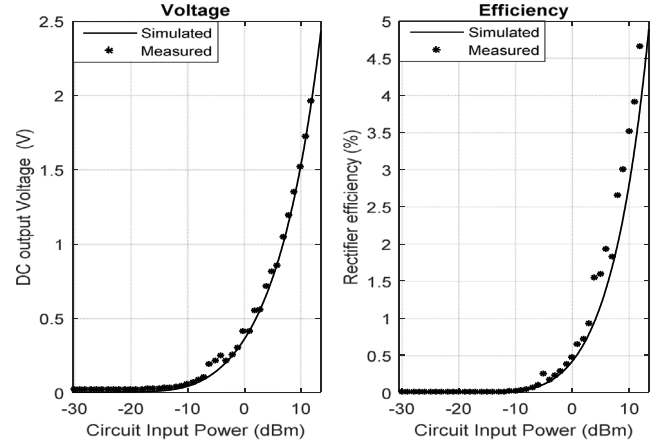
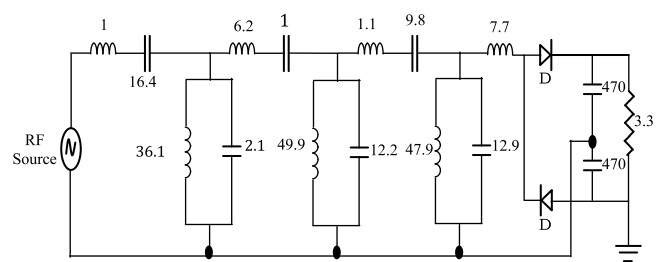
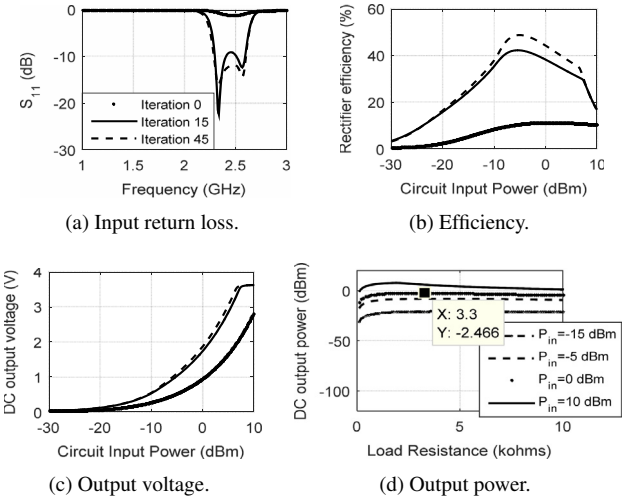
(a) Efficiency versus load resistance for  $V_{dc} = 1$  V.

(b) Detection threshold of the diodes.

**Fig. 3.** Comparison of the diode's performance.**Fig. 4.** Experimental setup.

be optimized according to our goals. A bandpass filter is considered here. The schema of the generated filter and rectifier circuit are shown in Fig. 6.

The optimization included in ADS software is used to find the best matching circuit and reach the better performance in

**Fig. 5.** Rectifier measurements results.**Fig. 6.** Rectifier with matching circuit.**Fig. 7.** Optimized rectifier performance.

terms of both efficiency and output voltage. The used optimization in this work is the gradient method search [13]. After designing a matching circuit, all components are optimized by setting two goals at the same time: minimizing return loss between 2.3 GHz and 2.6 GHz, and maximizing the DC output voltage.

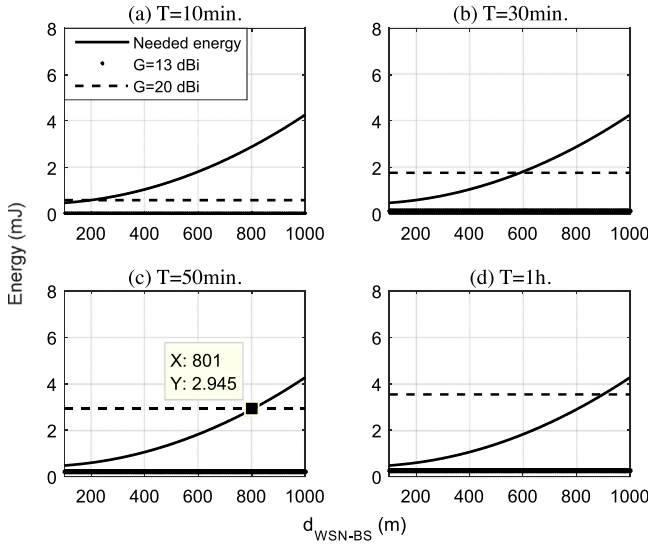
The results obtained after 45 iterations are shown in Fig. 7.

For an input power of 0 dBm, a 1.85 V output voltage is reached (Fig. 7(c)). A maximum conversion efficiency of 49%

**Table 3**

Summary of London RF survey measurements [14].

Band	Frequencies (MHz)	Maximum power density $S$ (nW/cm <sup>2</sup> )
DTV (during switch over)	470–610	460
GSM900 (MTx)	880–915	39
GSM900 (BTx)	925–960	1930
GSM1800 (MTx)	1710–1785	20
GSM1800 (BTx)	1805–1880	6390
3G (MTx)	1920–1980	66
3G (BTx)	2110–2170	240
WiFi	2400–2500	6

**Fig. 8.** Performance evaluation of the sensor node depending on receiving antenna gain.

is reached at around  $-5$  dBm. The component values to achieve these performances are shown in Fig. 6. The inductances are expressed in  $\mu H$ , the capacitors in  $pF$  and the resistances in  $k\Omega$ . Fig. 7(d) shows that the optimal load changes with the RF input power. At  $0$  dBm of input power, a maximum of  $-2.466$  dBm ( $0.57$  mW) is reached for optimum load resistance of  $3.3$  k $\Omega$ .

### 3.4. Performance evaluation of the sensor node

Assuming that all the recovered power is dedicated to the operation of the sensor node, the available energy ( $E_{\text{rec}}$ ) during a time  $T$  is defined as:

$$E_{\text{rec}} = P_{\text{max}} T \quad (9)$$

where  $P_{\text{max}}$  is the maximum recoverable power. The sensor node can operate only if ( $E_{\text{rec}} \geq E_{\text{node}}$ ).

To estimate the performance of the sensor node in a real environment, the spectral density measured in the Wi-Fi band and proposed in [14] is considered. In this previous work, these authors have made measurements of power density in the city of London, U.K. Measurements were made within the ultrahigh frequency (0.3–3 GHz) part of the frequency

spectrum. The results obtained in the different frequency bands are remembered in Table 3.

Assuming that the midband antenna gain is constant with frequency [15], the input RF power can be calculated by:

$$P_{RF} = S \cdot A_{\text{real}} \approx S \cdot G(f_0) \frac{\lambda_0^2}{4\pi} \quad (10)$$

where  $A_{\text{real}}$  is the capture area of the antenna,  $\lambda_0$  is the free-space wavelength at the midband frequency  $f_0$  and  $G(f_0)$  is the gain of the receiving antenna at  $f_0$ . Fig. 8 represents the performance of the sensor node depending on the gain of the receiving antenna and the minimum distance at which the WSN should be deployed to the BS to enslave the sensor node at the recovered energy. For our experiments,  $M = 100$  m,  $N = 100$ ,  $E_{\text{elec}} = 50$  nJ/bit,  $\varepsilon_{fs} = 10$  pJ/bit/m<sup>2</sup>,  $\varepsilon_{amp} = 0.0013$  pJ/bit/m<sup>4</sup>,  $E_{DA} = 5$  nJ/bit/signal;  $\ell = 4200$  bits and  $0 \leq d_{\text{WSN-BS}} \leq 1000$ .

Given the small amounts of recoverable power, it is necessary to use high gain antennas.

- If each round is performed every 10 min (Fig. 8(a)), it is necessary to deploy the WSN only at 216 m from the BS.
- Fig. 8(b) shows that the WSN should be deployed at 591 m from the BS for measurements to be performed every 30 min.
- For measurements performed every 50 min (Fig. 8(c)), the WSN can be deployed at 800 m from the BS.
- Fig. 8(d) considers the case of measurements to be made every hour, as changes in ambient temperature happening very slowly because of the thermal inertia. The WSN can be located at 900 m from the BS.

### 4. Conclusion

In this paper, a new method for autonomous WSN design powered by RF energy is proposed. The method consists of enslaving the WSN nodes to the amount of the available energy. The distance separating the WSN from the base station is used as the enslavement parameter. The obtained results show that, at  $0$  dBm ambient RF power, a WSN with  $100 \times 100$  m<sup>2</sup> distributed nodes – over an area of  $100$  – can be deployed at 800 m from the base station when the controlled physical quantity is sent every 50 min.

Although the obtained results validate the use of electromagnetic waves as an alternative energy source for sensor nodes (in remote areas), improvements are still possible. For instance, it is possible to consider radio modules operating in the GSM band

rather than the ISM band since the 900 MHz GSM band has been known to have a better power density.

### Conflict of interest

The authors declare that there is no conflict of interest in this paper'.

### References

- [1] V.J. Hodge, S. O'Keefe, M. Weeks, A. Moulds, Wireless sensor networks for condition monitoring in the railway industry: A survey, *IEEE Trans. Intell. Transp. Syst.* 16 (3) (2015) 1088–1106.
- [2] A. More, S. Wagh, K. Joshi, A test-bed for habitat monitoring system using Wi-Fi in Wireless Sensor Networks, in: IEEE International Conference on Computational Intelligence and Computing Research, ICCIC, Madurai, 2015, pp. 1–6.
- [3] I. Mohd Noor, M.R. Yuce, Review of medical implant communication system (MICS) band and network, *ICT Express* 2 (4) (2016) 188–194.
- [4] Q. Chi, H. Yan, C. Zhang, Z. Pan, L. Da Xu, A reconfigurable smart sensor interface for industrial WSN in IoT environment, *IEEE Trans. Ind. Inf.* 10 (2) (2014) 1417–1425.
- [5] S. Sudevalayam, P. Kulkarni, Energy harvesting sensor nodes: Survey and implications, *IEEE Commun. Surv. Tutor.* 13 (3) (2010) 443–461.
- [6] V.C. Gungor, G.P. Hancke, Industrial wireless sensor networks: Challenges, design principles, and technical approaches, *IEEE Trans. Ind. Electron.* 56 (2009) 4258–4265.
- [7] W.B. Heinzelman, A.P. Chandrakasan, H. Balakrishnan, An application-specific protocol architecture for wireless microsensor networks, *IEEE Trans. Wirel. Commun.* 1 (4) (2002) 660–670.
- [8] V.P. Mhatre, C. Rosenberg, D. Kofman, R. Mazumdar, N. Shroff, A minimum cost heterogeneous sensor network with a lifetime constraint, *IEEE Trans. Mob. Comput.* 4 (1) (2005) 4–15.
- [9] V. Shnayder, M. Hempstead, B.R. Chen, G.W. Allen, M. Welsh, Simulating the power consumption of large-scale sensor network applications, in: Proceedings of the 2nd International Conference on Embedded Networked Sensor Systems, Baltimore, 2004, pp. 188–200.
- [10] A. Mouapi, N. Hakem, Enslavement of wireless sensor network to an RF energy harvesting system, *Open J. Antennas and Propagation* 5 (02) (2017) 63–82.
- [11] A. Chang-Jun, An applicable 5.8 GHz wireless power transmission system with rough beamforming to Project Loon, *ICT Express* 2 (2) (2016) 87–90.
- [12] J.O. McSpadden, L. Fan, K. Chang, Design and experiments of a high-conversion-efficiency 5.8-GHz rectenna, *IEEE Trans. Microw. Theory Tech.* 46 (12) (1998) 2053–2060.
- [13] W.W. Hager, H. Zhang, A new conjugate gradient method with guaranteed descent and an efficient line search, *SIAM J. Optim.* 16 (1) (2005) 170–192.
- [14] M. Piñuela, P.D. Mitcheson, S. Lucyszyns, Ambient RF energy harvesting in urban and semi-urban environments, *IEEE Trans. Microw. Theory Tech.* 61 (7) (2013) 2715–2726.
- [15] C.C. Chen, J.L. Volakis, Ultrawide Bandwidth Antenna Design, in: *Antenna Engineering Handbook*, 2007.